NUCLEAR INSTRUMENTS AND METHODS 98 (1972) 413–417; © NORTH-HOLLAND PUBLISHING CO.

IMPROVED COMPUTER SIMULATION OF THE DETECTION PROCESS IN NE-102 AND NE-213 SCINTILLATORS FOR 0 TO 4.8 MeV NEUTRONS*

W. W. LINDSTROM† and B. D. ANDERSON

Case Western Reserve University, Cleveland, Ohio 44106, U.S.A.

Received 24 September 1971

A description is given of a FORTRAN subroutine which, in conjunction with a Monte-Carlo main program, accurately simulates the experimentally observed variation of detector efficiency with neutron energy throughout the discriminator cut-off region. With absolute C(n,n) and H(n,n) cross sections supplied, the program permits determination of the absolute detection efficiency from measurements of relative detection efficiency in this cut-off region. Variations of detector efficiency with incident neutron entry point and direction are also obtainable.

1. Introduction

Neutron detection efficiencies are required for both yield and polarization measurements. Yield measurements require efficiency *averaged* over the detector, whereas calculation of neutron polarimeter analyzing power requires knowledge of the relative efficiency as a function of the *direction* and *point of entry* of the incident neutron as well. The FORTRAN subroutine DETEFF described below can perform both of the above calculations, by calling it from different main programs. Input parameters for DETEFF are the incident neutron energy, entry point, and direction. Its output, when averaged over many subroutine calls, is the detection probability corresponding to that set of input parameters.

Such a computer program has been published[1]), and the purpose of the present paper is to describe three major modifications made to this previous program. The most important of these is the inclusion of the scintillator–photomultiplier resolution, which yields accurate simulation of the experimentally observed variation of detector efficiency with neutron energy throughout the discriminator cut-off region. Recent data for the light output from recoil protons in NE-102 and NE-213 scintillators+ are also incorporated, as well as a more detailed simulation of the C(n,n) angular distributions.

2. Program modifications

2.1. Scintillator–photomultiplier resolution

Prescott[2]) has shown that the observed distribution of photomultiplier output pulse heights can be described by a convolution of a Poisson distribution of photoelectron production and a binomial distribution of photomultiplier gain. We have found, however, that it is not necessary to generate such complicated functions. The observed distributions can be fitted as well by simple Poisson distributions, if the "photoelectron" axis is expanded by a factor of 1.53 to account for the photomultiplier gain spread.

Fig. 1 shows a Poisson distribution, as generated in the program, with the observed photomultiplier output for an average of 7.8 photoelectrons, as quoted by Prescott[2]). The smoothed, discrete Poisson distribution was generated for an average of 7.8/1.53 = 5.1 photoelectrons and then expanded on the pulse height axis by the same factor 1.53, with its area held constant at 1. Equally good fits are obtained for other pulse heights. Use of this phenomenological fit greatly simplifies the program.

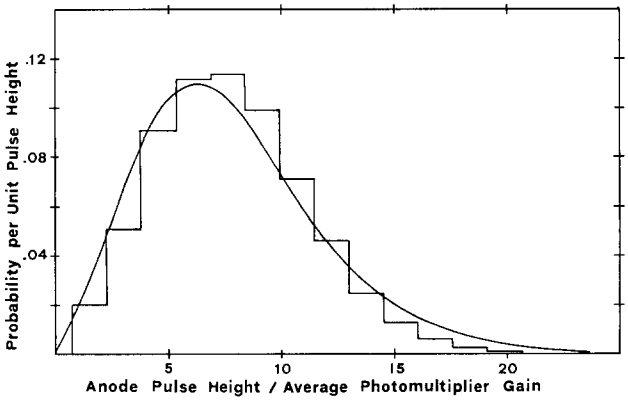

Fig. 1. Comparison of program simulation (histogram) with the observed (smooth curve) photomultiplier pulse-height distribution for an average of 7.8 photoelectrons.

* Research supported in part by the U.S. Atomic Energy Commission.

† Present address: Department of Physics, University of Basel, Switzerland.

+ Supplied by Nuclear Enterprises, Ltd., Winnipeg, Canada.

2.2. Detailed C(n,n) angular distribution

Published data[3–5]) have been used to generate inverse distribution function matrices to simulate C(n,n) elastic-scattering angular distributions. Forty-nine inverse distribution function arrays of 30 elements each have been generated to span a neutron energy range of 0 to 4.8 MeV (lab) in 0.1 MeV steps. In addition, thirty-five additional arrays expand the energy regions around the resonances at 2.082 MeV and 2.96 MeV in finer energy meshes of 1 and 20 keV, respectively.

Fig. 2 shows a histogram of the program output for comparison with the observed[3]) angular distribution at 2.083 MeV.

2.3. Recoil particle light-output formulae

The dependence of the photomultiplier pulse-height upon the energy of proton recoils, which is in strong disagreement with ref. 1, was obtained from recent data of Smith et al.[6]). Carbon recoil pulse heights were obtained by extrapolation of data of Steuer and Wenzel[7]).

Relations used in the program were:

for NE-213 scintillator

Average pulse height from photon recoils =

$= 0.0914\,E_p$, $(E_p < 0.4$ MeV),

$= 0.0144 + 0.1385\,E_p^2$, (0.4 to 0.9 MeV),

$= -0.0940 + 0.2450\,E_p$, (0.9 to 1.2 MeV),

$= -0.3626 + 0.4688\,E_p$, (1.2 to 2.0 MeV),

$= -0.5804 + 0.5777\,E_p$, (2.0 to 3.6 MeV),

$= -1.0440 + 0.7065\,E_p$, $(E_p > 3.6$ MeV),

Average pulse height from carbon recoils =

$= 0.006\,E_C + 0.00044\,E_C^2$,

and for NE-102 scintillator

Average pulse height from proton recoils =

$= 0.0735\,E_p + 0.0787\,E_p^4$, $(E_p < 1.05$ MeV),

$= 0.1608\,E_p^{(1.557)}$, $(E_p > 1.05$ MeV),

Average pulse height from carbon recoils =

$= 0.016\,E_C + 0.0004\,E_C^2$,

with the recoil energies E_p and E_C in MeV and the average pulse height from stopped 1 MeV electrons being one pulse height unit. The proton formulae are not valid above $E_p = 10$ MeV (9 MeV) for NE-213 (NE-102) and the carbon formulae are not valid above $E_C = 5$ MeV, but for our purpose this does not matter since neglect of inelastic processes limits the program use to incident neutron energies less than 4.8 MeV in any event.

3. Subroutine logic flow

Fig. 3 shows a flow chart of the resulting subroutine. Much of the excellent, detailed discussion of the original program[1]) still applies, and will not be repeated here. The only *logical* difference (shown in the dashed rectangle in the lower left-hand corner) is the introduction of a statistical distribution of photomultiplier pulse heights for identical charged-particle energy losses in the scintillator. Instead of assigning a fixed amount of anode charge ("light" in ref. 1) to each proton or carbon recoil of definite energy, the scintillator-photomultiplier resolution has been simulated, as explained in section 2.2, above. This procedure is obviously more realistic, since pulse-height resolutions (fwhm/peak) of 30% are common at the thresholds used in many experiments.

As in the original program, the energy E, position X, Y, Z, direction cosines U, V, W, and arrival weight *ARIVWT* of a single weighted neutron are supplied to the subroutine. *ARIVWT*, which permits general use of the subroutine in weighted Monte-Carlo main programs, was always set to 1 in the present work.

The current or "running" values of detected charge *PE*, accumulated neutron weight *ACUMWT*, and time-after-entry *TIMENS* are initialized to 0, 1, and 0, respectively. A minimum energy requirement of 10 keV

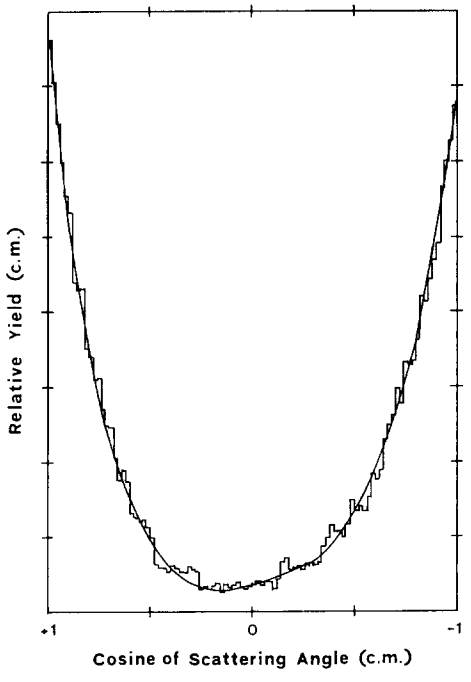

Fig. 2. Comparison of program simulation (histogram) of the C(n,n) angular distribution at $E_n = 2.083$ MeV with data (smooth curve) supplied as program input.

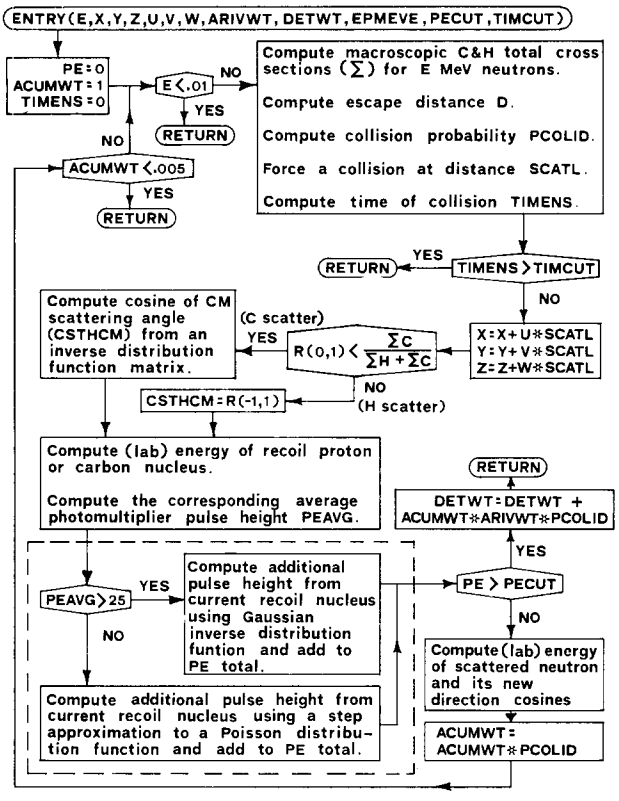

Fig. 3. Flow chart for subroutine DETEFF.

eliminates wasteful program "looping" for neutrons with insufficient energy for detection. The neutron is assigned a weight *PCOLID* equal to its probability of colliding with either C or H nuclei before leaving the detector volume, and a collision site is randomly selected. A maximum time requirement eliminates events outside the detector integration time *TIMCUT*, for this work 1000 ns. Updating of the neutron position is followed by random selection of the recoil nucleus (C or H) and the direction of neutron scattering (see section 2.2). Assuming total scintillator absorption of the recoil nucleus energy, the average detected charge *PEAVG* is obtained (see section 2.3).

Simulation of detector resolution depends upon pulse height. If *PEAVG* is not greater than 25, the detected charge *PE* is chosen randomly from a step Poisson distribution of average *PEAVG* (see section 2.1). If *PEAVG* is greater than 25 a Gaussian inverse distribution function matrix is randomly interrogated to yield the contribution to *PE*, saving computation time. In either case, the total PE is compared with a threshold value *PECUT* to see if it is sufficient to "trigger the detector discriminator". If so, the detected neutron weight *DETWT* is increased by the current neutron weight *ACUMWT* * *ARIVWT* * *PCOLID* and the subroutine returns to the calling program.

If *PE* is not greater than *PECUT*, the current neutron energy *E* and direction *U*, *V*, *W* are set equal to those of the newly scattered neutron, and the accumulated neutron weight *ACUMWT* is updated. The subroutine is then recycled, using the current values of *E*, *X*, *Y*, *Z*, *U*, *V*, *W*, *PE*, *ACUMWT* and *TIMENS*.

The requirements of *E* not less than 10 keV, *TIMENS* not greater than *TIMCUT* and *ACUMWT* not less than 0.005 have been inserted to minimize unnecessary computation time. They do limit the validity of the results for very low neutron energies, scintillators with very low light decay, and very low detector efficiencies. These effects are all quite negligible for the present work (see figs. 4 and 5). In fact, a tightening of these requirements would most probably decrease the computation time while negligibly influencing the result.

4. Subroutine operation

Operation of the subroutine with a main program is

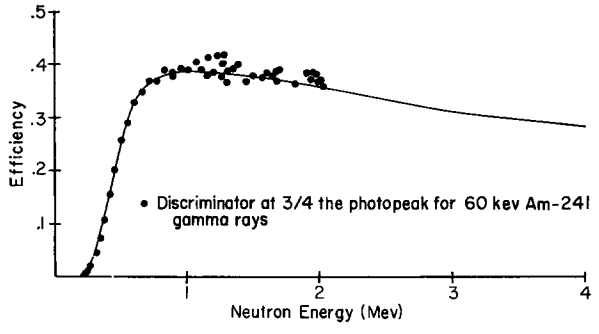

Fig. 4. Comparison of measured relative efficiency (data points) and calculated absolute efficiency (solid lines) for an NE-213 detector cylinder, 5.08 cm diam. × 5.08 cm high, uniformly illuminated perpendicular to its axis.

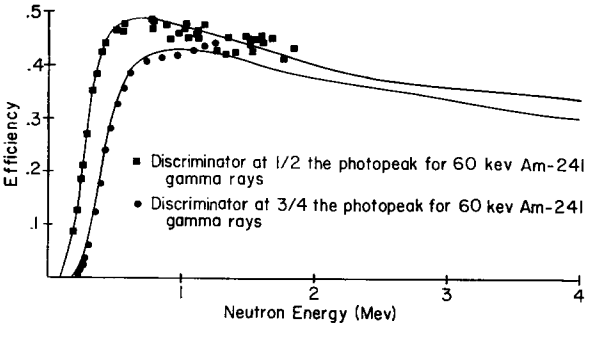

Fig. 5. Comparison of measured relative efficiency (data points) and calculated absolute efficiency (solid lines) for an NE-102 detector cylinder, 5.08 cm diam. × 5.08 cm high, uniformly illuminated perpendicular to its axis.

straightforward. To calculate the detector efficiency for a given neutron illumination profile (in both energy and space), the calling program need only simulate such an ensemble of neutrons as they strike the detector, one-by-one.

The parameter *PECUT* is chosen to simulate the detector resolution. For each scintillator-photomultiplier combination, the pulse height distribution of the total absorption peak from 60 keV ^{241}Am gamma rays was observed. In our case, a smoothed Poisson distribution with an average of 18.5 (18.0) "photoelectrons[8])" was found to have the same resolution as this peak for NE-213 (NE-102). *PECUT* is set proportional to the detector threshold used; an NE-102 detector threshold at $\frac{1}{2}$ the ^{241}Am peak required a *PECUT* of 9.0, for example.

The parameter *EPMEVE* is the conversion factor from the light output formulae, for which stopped 1 MeV electrons are arbitrarily assigned unit pulse height, to the detector pulse height, which has the same units as *PECUT*. *EPMEVE* is varied until the rapid rise in detector efficiency just above cut-off is simulated. This requires, of course, a measurement of the relative neutron detection efficiency throughout this cut-off region.

5. Results

Figs. 4 and 5 show the ability of the program to fit the observed relative efficiency of 5.08 cm diam. × 5.08 cm thick cylinders of NE-213 and NE-102 uniformly illuminated perpendicular to their axes.

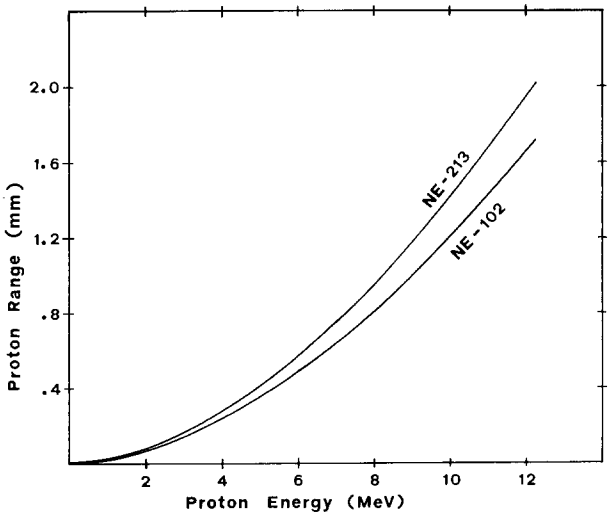

Fig. 6. Calculated proton ranges in NE-213 and NE-102 scintillator.

Efficiency data for both scintillators were obtained simultaneously, using neutrons from the T(p,n)^{3}He reaction and the differential cross section data of Jarvis et al.[9]) with the same tritium gas target filling, etc. Thus the ratios of Ne-213 and NE-102 detector efficiencies are predicted absolutely by the program, which contains the known scintillator densities and H/C ratios. The *same* scale factor was therefore used in both relative efficiency plots; it was chosen for best overlap with the NE-213 absolute efficiency predictions.

Agreement of the program predictions with the observed efficiencies is seen to be excellent. The accurate simulation of the efficiency ratios for different scintillators and different discriminator biases, as well as the shapes near threshold, gives one confidence that the major physical processes are being handled correctly.

As in ref. 1, we have neglected the "edge effects" of recoiling nuclei escaping from the scintillator before losing sufficient energy to be detected. The detector resolution part of the program, with the same parameters used to calculate fig. 4, was used to provide an estilate of such losses. Fig. 6 shows the calculated ranges of recoil protons in NE-213 and NE-102 scintillator. An 8 MeV proton is seen to travel 0.025 mm in NE-213 while slowing down to 7.9 MeV, and this energy loss yields an anode pulse equivalent to that of a stopped 0.53 MeV proton[6]). Calculations show that detection of such events is 90% certain. Thus an 8 MeV proton must be produced within 0.025 mm of the scintillator surface to have an appreciable chance to escape detection. Since this region encompasses only 0.24% of the volume of our detectors, and since less than $\frac{1}{2}$ of such recoils will be directed toward the surface, such losses amount to at most 0.1% at 8 MeV, and will be less for lower energies.

One interesting by-product of this investigation deserves mention. The precise inclusion of the C(n,n) resonance at 2.082 MeV was found to be unimportant. It was at first thought that this strongly forward–backward peaked $l = 2$ resonance would cause a pronounced dip in the neutron detection efficiency – by ejecting a greater percentage of incoming neutrons directly opposite to their original path, and out of the front face of the detector – than would a more nearly isotropic scattering. A slight efficiency dip was computed, but it was at most a 2% effect and was limited to a 6 keV energy range. For the 30 keV neutron energy spreads commonly encountered in experimental work, a reduction of only 0.4% would be expected.

The authors would like to express their gratitude to Dr. E. F. Shrader for his continued interest and

support, and to Dr. P. R. Bevington for his generous help with the computerology and for his incisive critical reading of the manuscript.

Listings of the subroutine and calling program are available for both NE-213 scintillator (subroutine DET213) and NE-102 scintillator (subroutine DET102) on request from the authors.

References

[1]) B. Gustafsson and O. Aspelund, Nucl. Instr. and Meth. **48** (1967) 77.

[2]) J. R. Prescott, Nucl. Instr. and Meth. **22** (1963) 256.

[3]) R. O. Lane, A. Langsdorf, Jr., J. E. Monahan and A. J. Elwyn, Tables of differential cross sections for scattering of neutrons from various nuclei (1960) unpublished.

[4]) J. E. Wills, Jr., J. K. Blair, H. O. Cohn and H. B. Willard, Phys. Rev. **109** (1958) 891.

[5]) R. J. Howerton, Tabulated differential neutron cross sections, UCRL-5573 (1961).

[6]) D. L. Smith, R. J. Polk and T. G. Miller, Nucl. Instr. and Meth. **64** (1968) 157.

[7]) M. F. Steuer and B. E. Wenzel, Nucl. Instr. and Meth. **33** (1965) 131.

[8]) Due to photomultiplier chain secondary emission fluctuations the actual number of photoelectrons emitted from the photocathode is greater than this. As shown in section 2.1, however, these two numbers are related by a constant factor, and this factor is automatically subsumed in the phenomenological choice of the factor EPMEVE, as described in the subsequent text.

[9]) G. A. Jarvis, A. Hemmendinger, H. V. Argo and R. F. Taschek, Phys. Rev. **79** (1950) 929.